Quantum simulation of many-body effects in steady-state nonequilibrium: Electron-phonon coupling in quantum dots

J. E. Han
Department of Physics, State University of New York at Buffalo, Buffalo, New York 14260, USA
(Received 20 September 2005; revised manuscript received 16 December 2005; published 15 March 2006)

We develope a method of mapping quantum nonequilibrium steady-state to an effective equilibrium system and present an algorithm to calculate electron-transport using an equilibrium technique. A systematic implementation of boundary conditions in steady-state nonequilibrium is made in the statistical operator $\hat{Y}$ constructed from scattering state operators. We explicitly demonstrate the equivalence of this method to nonequilibrium Green function techniques for a noninteracting quantum dot model. In electron-phonon coupled quantum dot systems, we formulate an algorithm to construct the statistical bias operator $\hat{Y}$ and perform a full many-body calculation with the quantum Monte Carlo technique. The results coherently demonstrate various transport behaviors such as phonon dephasing, $I-V$ staircase, and phonon-assisted tunneling phenomena. This formulation makes the existing computational quantum many-body techniques applicable to quantum steady-state nonequilibrium problems, which will complement the theories based on the diagrammatic approach.

DOI: 10.1103/PhysRevB.73.125319 PACS number(s): 73.63.Kv, 72.10.Bg, 72.10.Di

I. INTRODUCTION

Electronic transport in nanoscale devices has recently attracted much attention for its tremendous impact in modern electronics. To advance today's nanoscale electronics, we are in an increasing need for understanding fundamental roles of quantum mechanical effects among interacting electrons and their statistical mechanics far from equilibrium. With an ever decreasing physical dimension of devices, many solid-state approaches have to be severely modified in the realm of a nanoscale device under extremely strong external fields.

Despite the intense research in the nanoscale transport, most of the theoretical tools used today are based on the Green function technique.[1–4] We note that powerful numerical many-body techniques, which have been essential in equilibrium quantum many-body theories, have not been useful due to the lack of understanding of the nonequilibrium ensemble. Possible application of the well-established numerical techniques, such as the quantum Monte Carlo method, exact diagonalization for example, to nonequilibrium systems will provide a breakthrough in the field. The goal of this work is to formulate a general scheme by combining the nonequilibrium theory with numerical quantum many-body techniques through mapping of a nonequilibrium system to an effective equilibrium. We first establish the method by explicitly solving the electron transport through a noninteracting quantum dot system using the equilibrium technique. We apply the method to an interacting system of an electron-phonon coupled quantum dot and reproduce various transport phenomena such as the phonon dephasing, phonon-assisted tunneling, and *I-V* staircase in a single framework. The formulation is applicable to other numerical techniques, such as the numerical renormalization group, exact diagonalization, etc.

The diagrammatic theory is based on an expansion of Green functions which describe the propagation of excitations as interactions are adiabatically turned on. Here, we start from a different observation that a steady-state nonequilibrium possesses the time invariance once the transient behavior dies out. As the starting point of the following nonequilibrium theory, our focus is mainly on the construction of the steady-state nonequilibrium ensemble, equivalently an operator governing its distribution, for a given boundary condition.

Zubarev[6] has generalized the Gibbsian statistical mechanics to the steady-state nonequilibrium and has established the quantum mechanical statistical operator method which incorporates nonequilibrium boundary conditions. In the context of the modern electronics, Hershfield[7] has shown the existence of a statistical operator $\hat{Y}$ which accounts for the nonequilibrium boundary condition as a part of an effective Hamiltonian. He proposed that $\hat{Y}$ be constructed in terms of the scattering state operators. The ensemble can be represented in terms of a modified partition function Z_{noneq} for nonequilibrium as

$$Z_{\text{noneq}} = \text{Tr}\, e^{-\beta(\hat{H}-\hat{Y})} \quad \text{with } \beta = 1/T, \tag{1}$$

where $\hat{H}$ is the Hamiltonian operator for the whole (open) system including the source (left, L), drain (right, R) reservoirs and quantum dot (QD) [see Fig. 1(a)]. The additional operator $\hat{Y}$ contains the boundary condition of multiple chemical potentials in the electronic reservoirs. The chemical potential difference between the source-drain reservoirs is given by Φ. Once the bias operator $\hat{Y}$ is constructed, one can apply the equilibrium QMC technique (or other equilibrium techniques) such as the finite-temperature path integral method[5] to $\hat{H}_{\text{noneq}}=\hat{H}-\hat{Y}$ as if $\hat{H}_{\text{noneq}}$ describes an equilibrium. To obtain *I-V* characteristics, for instance, one simply needs to evaluate the expectation value of the current operator $\hat{I}$,

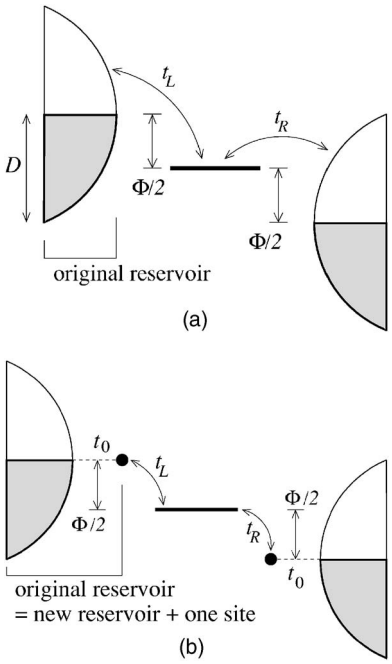

FIG. 1. (a) Schematic diagram of a quantum transport device. The source and drain reservoirs are biased by a chemical potential difference Φ. The quantum dot (QD) level is set in the middle for simplicity. (b) Each reservoir is mapped to a single site and a new reservoir. The three discrete sites for the QD, L, and R sites are treated in a fully quantum mechanical manner.

$$I = \frac{\mathrm{Tr}\,\hat{I}e^{-\beta(\hat{H}-\hat{Y})}}{\mathrm{Tr}\,e^{-\beta(\hat{H}-\hat{Y})}} = -\frac{ie}{h}\sum_{k\sigma}\frac{t_{Lk}}{\sqrt{\Omega}}[\langle d_\sigma^\dagger c_{Lk\sigma}\rangle - \langle c_{Lk\sigma}^\dagger d_\sigma\rangle], \quad (2)$$

where $c_{Lk\sigma}^\dagger$ ($c_{Lk\sigma}$) is the electron creation (annihilation) operator of the kth continuum state in the L reservoir with spin σ, $d_\sigma^\dagger$ (d_σ) as the operator for the QD state, and t_α ($\alpha = L,R$) as the hopping integral (with volume Ω) between the QD and the α reservoir [see Fig. 1(a)].

II. FORMULATION

The central challenge is to construct the bias operator $\hat{Y}$. The condition that $\hat{Y}$ must fulfill is that $\hat{Y}$ is compatible with the time invariance of steady state. Once a nonequilibrium ensemble is established via $e^{-\beta(\hat{H}-\hat{Y})}$, the subsequent motion is governed by the time evolution operator $e^{-i\hat{H}t}$. Therefore the bias operator $\hat{Y}$ must satisfy the commutation relation $[\hat{H},\hat{Y}]=0$ to guarantee a steady-state ensemble. Hershfield[7] has shown that the problem can be solved by writing $\hat{Y}$ in terms of the scattering state operator $\psi_{\alpha k\sigma}^\dagger$ ($\alpha=L,R$) as[8]

$$\hat{Y} = \frac{\Phi}{2}\sum_{k\sigma}(\psi_{Lk\sigma}^\dagger\psi_{Lk\sigma} - \psi_{Rk\sigma}^\dagger\psi_{Rk\sigma}). \quad (3)$$

As depicted in Fig. 1(a), we choose to move the energy levels of the source and drain reservoirs with the shifted chemical potentials. We consider a simplified case of symmetric voltage drop.

The scattering state creation operator $\psi_{\alpha k\sigma}^\dagger$ satisfies the Lippman-Schwinger equation[9] in the operator form

$$\psi_{\alpha k\sigma}^\dagger = c_{\alpha k\sigma}^\dagger + \frac{1}{\epsilon_{\alpha k} - \mathcal{L}_0 + i\eta}[\hat{V},\psi_{\alpha k\sigma}^\dagger], \quad (4)$$

with $\epsilon_{\alpha k}$ is the asymptotic continuum energy and η is an infinitesimal convergence factor. The Liouville operator $\mathcal{L}_0$ for the noninteracting Hamiltonian $\hat{H}_0$ is defined as $\mathcal{L}_0\hat{A} = [\hat{H}_0,\hat{A}]$ when acted on an arbitrary operator $\hat{A}$. The interaction part of the Hamiltonian $\hat{V}$ ($\hat{H}=\hat{H}_0+\hat{V}$) includes the tunneling to a QD and many-body interactions. The above equation can be rewritten into the following Heisenberg equation:

$$[\hat{H},\psi_{\alpha k\sigma}^\dagger] = \epsilon_{\alpha k}\psi_{\alpha k\sigma}^\dagger + i\eta(\psi_{\alpha k\sigma}^\dagger - c_{\alpha k\sigma}^\dagger). \quad (5)$$

Due to the convergence factor $i\eta$ which fixes the boundary condition of the wave function at the infinite past, the above Heisenberg equation no longer has the time-reversal symmetry.

A. Noninteracting system

To demonstrate how to map a nonequilibrium ensemble to an effective equilibrium, we first consider a noninteracting system with the Hamiltonian $\hat{H}=\hat{H}_0+\hat{V}_t$, where $\hat{H}_0$ is the unperturbed Hamiltonian with disconnected reservoirs and a QD,

$$\hat{H}_0 = \sum_{\alpha k}\epsilon_{\alpha k}c_{\alpha k}^\dagger c_{\alpha k} + \epsilon_d d^\dagger d, \quad (6)$$

and $\hat{V}_t$ is the tunneling Hamiltonian between the reservoirs and the QD,

$$\hat{V}_t = \sum_{\alpha k}\frac{t_{\alpha k}}{\sqrt{\Omega}}(d^\dagger c_{\alpha k} + c_{\alpha k}^\dagger d). \quad (7)$$

Note that we have suppressed the spin degree of freedom. With the noninteracting Hamiltonian, the scattering state operator $\psi_{\alpha k}^\dagger$ can be expanded within the one-particle basis $\{c_{\alpha k}^\dagger, d^\dagger\}$ as

$$\psi_{\alpha k}^\dagger = c_{\alpha k}^\dagger + \gamma_d^{\alpha k}d^\dagger + \sum_{\beta k'}\gamma_{\beta k'}^{\alpha k}c_{\beta k'}^\dagger. \quad (8)$$

By substituting this to the Heisenberg equation Eq. (5) we obtain

$$\psi_{\alpha k}^\dagger = c_{\alpha k}^\dagger + \frac{t_{\alpha k}}{\sqrt{\Omega}}g_d^0(\epsilon_{\alpha k})\left[d^\dagger + \sum_{\beta k'}\frac{t_{\beta k'}}{\sqrt{\Omega}}\frac{c_{\beta k'}^\dagger}{\epsilon_{\alpha k} - \epsilon_{\beta k'} + i\eta}\right], \quad (9)$$

where $g_d^0(\epsilon)$ is the retarded Green function for the QD level

$$g_d^0(\epsilon) = \left(\epsilon - \epsilon_d - \frac{1}{\Omega}\sum_{\alpha k}\frac{|t_{\alpha k}|^2}{\epsilon - \epsilon_{\alpha k} + i\eta}\right)^{-1}. \quad (10)$$

In the large bandwidth limit[8], no localized states form outside the band continuum and one can readily show for noninteracting systems[9] that

$$\{\psi^{\dagger}_{\alpha k}, \psi^{\dagger}_{\beta k'}\} = \delta_{\alpha\beta}\delta_{kk'}, \tag{11}$$

$$\sum_{\alpha k} \psi^{\dagger}_{\alpha k}\psi_{\alpha k} = \sum_{\alpha k} c^{\dagger}_{\alpha k}c_{\alpha k} + d^{\dagger}d, \tag{12}$$

$$\sum_{\alpha k} \epsilon_{\alpha k}\psi^{\dagger}_{\alpha k}\psi_{\alpha k} = \hat{H}. \tag{13}$$

The bias operator $\hat{Y}$ in the noninteracting limit is then obtained via Eq. (3). Analytic calculation becomes particularly simple in the large bandwidth limit

$$\hat{Y} = \frac{\Phi}{2}\Bigg\{ \sum_k (c^{\dagger}_{Lk}c_{Lk} - c^{\dagger}_{Rk}c_{Rk}) + \frac{\Gamma_L - \Gamma_R}{\Gamma_L + \Gamma_R} d^{\dagger}d + \frac{2}{\sqrt{\Omega}}\sum_k \left[\frac{t_L\Gamma_R g^{0*}_d(\epsilon_{Lk})}{\Gamma_L + \Gamma_R} c^{\dagger}_{Lk}d - \frac{t_R\Gamma_L g^{0*}_d(\epsilon_{Rk})}{\Gamma_L + \Gamma_R} c^{\dagger}_{Rk}d + \text{h.c.} \right] + \sum_{\alpha\beta,kk'} S(\alpha k, \beta k') c^{\dagger}_{\alpha k}c_{\beta k'} \Bigg\}, \tag{14}$$

where the scattering matrix $\mathbf{S}$ is given as

$$S(\alpha k, \alpha k') = (-)^{\alpha} \frac{2\Gamma_L\Gamma_R}{\Omega \pi N(0)\Gamma} \frac{g^{0*}_d(\epsilon_{\alpha k}) - g^{0}_d(\epsilon_{\alpha k'})}{\epsilon_{\alpha k} - \epsilon_{\alpha k'} - i\eta}, \tag{15}$$

$$S(Lk, Rk') = \frac{2t_L t_R}{\Omega\Gamma} \frac{\Gamma_L g^{0*}_d(\epsilon_{Lk}) - \Gamma_R g^{0}_d(\epsilon_{Rk'})}{\epsilon_{Lk} - \epsilon_{Rk'} - i\eta}. \tag{16}$$

$\Gamma_{\alpha} = \Omega^{-1}\Sigma_k \pi |t_{\alpha k}|^2 \delta(\epsilon - \epsilon_{\alpha k})|_{\epsilon=\epsilon_F}$, $\Gamma = \Gamma_L + \Gamma_R$ and the sign $(-)^{\alpha}$ is defined as $(-)^L = 1$ and $(-)^R = -1$. In the flatband limit, the retarded QD Green function can be written as $g^0_d(\epsilon) = (\epsilon - \epsilon_d + i\Gamma)^{-1}$.

Now we demonstrate that the current can be computed within the equilibrium formalism by using $\hat{H} - \hat{Y}$ as the effective Hamiltonian. First, the QD Green function $G_d(i\omega_n)$ is computed at Matsubara frequency, $\omega_n = \pi(2n+1)/\beta$, as

$$G_d(i\omega_n) = \left\langle d \frac{1}{i\omega_n - \mathcal{L}_{H-Y}} d^{\dagger} \right\rangle - \left\langle d^{\dagger} \frac{1}{-i\omega_n - \mathcal{L}_{H-Y}} d \right\rangle, \tag{17}$$

where $\mathcal{L}_{H-Y}$ is the Liouville operator corresponding to $\hat{H} - \hat{Y}$. Throughout this paper, a Green function denoted by a lower-case letter such as $g^0_d(\epsilon)$ is a propagator with the time evolution given by $\hat{H}$, while a Green function denoted by an upper-case letter such as $G^0_d(i\omega_n)$ is with the time evolution by $\hat{H} - \hat{Y}$. In the noninteracting limit, $G_d(i\omega_n)$ can be easily calculated by using the spectral representation in terms of the complete set of $\psi^{\dagger}_{\alpha k}$ as

$$\left\langle d \frac{1}{i\omega_n - \mathcal{L}_{H-Y}} d^{\dagger} \right\rangle = \sum_{\alpha k}{}' \frac{\langle d|\psi_{\alpha k}\rangle\langle\psi_{\alpha k}|d\rangle}{i\omega_n - \epsilon_{\alpha k} + (-)^{\alpha}\Phi/2}, \tag{18}$$

with $\langle d|\psi_{\alpha k}\rangle = t_{\alpha k} g^0_d(\epsilon_{\alpha k})/\sqrt{\Omega}$ from Eq. (9). The above summation is performed over empty continuum states. After the second term in Eq. (17) is evaluated in the same manner with a summation over filled continuum states, we obtain for $\omega_n > 0$,

$$G_d(i\omega_n) = \frac{\Gamma_L/\Gamma}{i\omega_n - \epsilon_d + \Phi/2 + i\Gamma} + \frac{\Gamma_R/\Gamma}{i\omega_n - \epsilon_d - \Phi/2 + i\Gamma}. \tag{19}$$

For $\omega_n < 0$, $G_d(i\omega_n) = [G_d(-i\omega_n)]^*$.

We evaluate $\langle d^{\dagger}c_{Lk}\rangle$ in Eq. (2) from the off-diagonal Green function $G_{Lk,d}(i\omega_n)$,

$$G_{Lk,d}(i\omega_n) = \left\langle c_{Lk} \frac{1}{i\omega_n - \mathcal{L}_{H-Y}} d^{\dagger} \right\rangle - \left\langle d^{\dagger} \frac{1}{-i\omega_n - \mathcal{L}_{H-Y}} c_{Lk} \right\rangle. \tag{20}$$

Using the same method as applied to calculate $G_d(i\omega_n)$, we obtain for $\omega_n > 0$ (see Appendix A for details)

$$-\frac{it_L}{\sqrt{\Omega}}\sum_k [G_{Lk,d}(i\omega_n) - G_{d,Lk}(i\omega_n)] = \frac{2\Gamma_L\Gamma_R}{\Gamma_L + \Gamma_R}\left(\frac{1}{i\omega_n - \epsilon_d + \Phi/2 + i\Gamma} - \frac{1}{i\omega_n - \epsilon_d - \Phi/2 + i\Gamma} \right). \tag{21}$$

Finally, by summing over the Matsubara frequency, we obtain the expression for the current, in agreement with the Landauer-Büttiker formula

$$I = \frac{e}{\hbar}\frac{1}{\beta}\sum_k \frac{it_L}{\sqrt{\Omega}}\sum_k [G_{d,Lk}(i\omega_n) - G_{Lk,d}(i\omega_n)] = \frac{2e}{\hbar}\frac{\Gamma_L\Gamma_R}{\Gamma_L + \Gamma_R}\int d\epsilon [f(\epsilon - \Phi/2) - f(\epsilon + \Phi/2)]\rho_d(\epsilon). \tag{22}$$

$f(\epsilon)$ is the Fermi-Dirac function and $\rho_d(\epsilon)$ is the QD spectral function $\rho_d(\epsilon) = (\Gamma/\pi)[(\epsilon - \epsilon_d)^2 + \Gamma^2]^{-1}$ for a flatband in the large bandwidth limit.

B. Quantum dot with electron-phonon interaction

There are two main issues to be resolved in order to implement the nonequilibrium formulation in the presence of many-body interaction.

(i) The scattering state has many-particle excitations such as electron-hole pairs, magnetic excitations and collective modes, and the scattering state creation operator $\psi^{\dagger}_{\alpha k}$, and consequently the bias operator $\hat{Y}$, has nontrivial many-particle terms in addition to the non-interacting limit, Eqs. (9) and (14).

(ii) Since the scattering state operator $\psi^{\dagger}_{\alpha k}$ is an eigenoperator of the total Hamiltonian, the many-body terms dress all one-particle operators $\{c^{\dagger}_{\alpha k}, d^{\dagger}\}$. Therefore, the product $\psi^{\dagger}_{\alpha k}\psi_{\alpha k}$ creates nonlocal interaction terms between essentially all possible combinations of creation/annihilation operators even though the original Hamiltonian contained only local interactions on the QD. Despite the potential of Hershfield's paper,[7] only limited developments[10,11] have been made so far due to such difficulties.

Now we discuss a procedure to overcome such difficulties in an example: electron-phonon (el-ph) coupled QD connected to two L(source), R(drain)-reservoirs. A spinless Hamiltonian for the system reads $\hat{H}=\hat{H}_{\rm el}+\hat{H}_{\rm ph}+\hat{H}_{\rm ep}$,

$$\hat{H}_{\rm el}=\sum_{\alpha k}\epsilon_{\alpha k}c_{\alpha k}^{\dagger}c_{\alpha k}+\epsilon_d d^{\dagger}d+\sum_{\alpha k}\frac{t_{\alpha k}}{\sqrt{\Omega}}(d^{\dagger}c_{\alpha k}+\text{h.c.}),$$

$$\hat{H}_{\rm ph}=\frac{1}{2}(p^2+\omega_{ph}^2\varphi^2),\quad \hat{H}_{\rm ep}=\alpha\varphi(d^{\dagger}d-\langle d^{\dagger}d\rangle), \tag{23}$$

where φ is the phonon amplitude of an Einstein phonon on the QD, p its conjugate momentum, ω_{ph} the phonon frequency, and $\alpha(\equiv g\sqrt{2\omega_{ph}})$ the el-ph coupling constant. As shown in Fig. 1(a), we model that the center of mass of the continuum states shifts with the bias, i.e., $\epsilon_{Lk}=\epsilon_k+\Phi/2$ and $\epsilon_{Rk}=\epsilon_k-\Phi/2$. We set the QD level in the middle of the two chemical potential ($\epsilon_d=0$) in the particle-hole symmetric limit for simplicity.

1. Truncation of nonlocal interactions

In order to develop a systematic treatment of the nonlocal interaction terms in $\hat{Y}$, we propose the following scheme. We make two main physical observations in the above $\hat{H}$ with the el-ph interaction. First, the QD level is modulated by phonons as $\epsilon_d(\varphi)=\epsilon_d+\alpha\varphi$. The quantum fluctuation of the QD level leads to the dephasing of current. Second, the hopping out of the QD to the continuum is effectively modified as $\epsilon_d(\varphi)$ is driven in and out of resonance with respect to the reservoir chemical potentials. As will be discussed later, fluctuations in the hopping integral lead to phonon satellite peaks in I-V characteristics, and therefore, it is crucial to take into account the full quantum mechanical effects on the QD and the first hopping sites.

We single out the quantum state with direct tunneling to the QD by rewriting the each continuum as composed of a fictitious site ($c_{\alpha}^{\dagger}=\sqrt{\Omega^{-1}\Sigma_k}c_{\alpha k}^{\dagger}$) and a new continuum, as sketched in Fig. 1(b). Since we treat the original continuum as noninteracting, the above decomposition can be made exactly. We then treat the coupling between the three sites $(d^{\dagger},c_L^{\dagger},c_R^{\dagger})$ fully quantum mechanically and make a mean-field approximation to the rest of the new continuum states. Since the strength of the non-local interaction in $\hat{Y}$ should decay as we go deeper into the reservoirs, this procedure will be systematically improved by increasing the number of fictitious sites.

In this work, we have used a semicircular density of states (DOS) for the continua, $N_{\alpha}(\epsilon)=2\sqrt{\{D^2-(\epsilon-(-)^{\alpha}\Phi/2)^2\}}/\pi D^2$, with the half-bandwidth D. The semicircular DOS is particularly useful since the continuum can be represented by a semi-infinite chain of a constant hopping integral $t_0=D/2$, thereby with the DOS of the new continuum identical to the original DOS.

2. Interacting scattering state operator $\psi_{\alpha k\sigma}^{\dagger}$

A good choice of $\psi_{\alpha k\sigma}^{\dagger}$, and subsequently the bias operator $\hat{Y}$, is crucial for a successful mapping of nonequilibrium system. Depending on the strength of many-particle interactions in $\hat{H}$, we have to choose an appropriate approximation in constructing the full scattering state $\psi_{\alpha k\sigma}^{\dagger}$. In our example of el-ph interaction with moderate electron correlations, $\psi_{\alpha k\sigma}^{\dagger}$ in the perturbation expansion about the el-ph coupling would be reasonable. We expect that the electron transport in the strongly correlated system, such as for the anomalous conductance in Kondo regime, requires a nonperturbative treatment of the interaction in the bias operator which goes beyond the treatment in this paper.

Here we follow the procedure sketched out in Hershfield's paper.[7] The full scattering state operator is expanded in terms of interaction strength, $\psi_{\alpha k\sigma}^{\dagger}=\Sigma_n\psi_{\alpha k\sigma,n}^{\dagger}$, where the nth term $\psi_{\alpha k\sigma,n}^{\dagger}$ is of the nth order perturbation. From the Heisenberg equation of motion, Eq. (5), we have a recursive relation

$$[\hat{H}_{\rm ep},\psi_{\alpha k\sigma,n-1}^{\dagger}]=(\epsilon_{\alpha k}+i\eta)\psi_{\alpha k\sigma,n}^{\dagger}-[\hat{H}_0,\psi_{\alpha k\sigma,n}^{\dagger}], \tag{24}$$

where $\hat{H}_0$ is now the unperturbed part, $\hat{H}_0=\hat{H}_{\rm el}+\hat{H}_{\rm ph}$.

The unperturbed scattering state operator $\psi_{\alpha k,0}$, Eq. (9), is now expressed in terms of the new basis set. The unperturbed retarded Green function with respect to the discrete basis $(d^{\dagger},c_L^{\dagger},c_R^{\dagger})$ can be easily obtained as

$$\boldsymbol{g}^0(\epsilon)=(\epsilon-\hat{H}+i\eta)^{-1}=\begin{bmatrix}\epsilon-\Sigma_L(\epsilon) & -t_L & 0\\ -t_L & \epsilon-\epsilon_d & -t_R\\ 0 & -t_R & \epsilon-\Sigma_R(\epsilon)\end{bmatrix}^{-1}, \tag{25}$$

where $\Sigma_{\alpha}(\epsilon)=\Omega^{-1}\Sigma_k|t_{\alpha k}|^2/(\epsilon-\epsilon_{\alpha k}+i\eta)$. Green functions involving continuum states can be written in terms of the above Green functions. For example, $g_{L,Lk}^0=g_{LL}^0(\epsilon)(t_{Lk}/\sqrt{\Omega})(\epsilon-\epsilon_{Lk}+i\eta)^{-1}$ and $g_{L,Rk}^0=g_{LR}^0(\epsilon)(t_{Rk}/\sqrt{\Omega})(\epsilon-\epsilon_{Rk}+i\eta)^{-1}$. Then $\psi_{\alpha k,0}$ in Eq. (9) can be equivalently written as

$$\psi_{Lk,0}^{\dagger}=c_{Lk}^{\dagger}+\frac{t_0}{\sqrt{\Omega}}\sum_{\beta}g_{L,\beta}^0(\epsilon_{Lk})c_{\beta}^{\dagger}, \tag{26}$$

where $\beta=Lk',L,d,R,Rk'$ with L, R denoting the fictitious reservoir sites, and Lk', Rk' denoting the continuum states. $c_{Lk}^{\dagger}$ is the incoming state of the new continuum and $c_d^{\dagger}$ is the same as $d^{\dagger}$.

Now we expand the scattering states up to the harmonic order of the el-ph coupling via Eq. (24). Since $[\hat{H}_{\rm ep},\psi_{Lk,0}^{\dagger}]=(t_0/\sqrt{\Omega})\alpha\varphi g_{Ld}^0(\epsilon_{Lk})d^{\dagger}$ is in the linear order of the fermionic operators, $\psi_{\alpha k,1}^{\dagger}$ can be expanded as

$$\psi_{Lk,1}^{\dagger}=\varphi\sum_{\beta}a_{\beta}^{Lk}c_{\beta}^{\dagger}+p\sum_{\beta}b_{\beta}^{Lk}c_{\beta}^{\dagger}. \tag{27}$$

Equation (24) with $n=1$ can be solved straightforwardly, with the explicit derivation provided in Appendix B. In this work, we stop at the order $n=1$.

The bias operator $\hat{Y}$ is calculated up to the linear order of (φ,p) in $\hat{Y}=\hat{Y}_0+\hat{Y}_1$ with $\hat{Y}_0$ given in Eq. (3) and $\psi_{\alpha k}^{\dagger}$ replaced by $\psi_{\alpha k0}^{\dagger}$ as

$$\hat{Y}_1 = \frac{\Phi}{2}\sum_k (\psi^\dagger_{Lk0}\psi_{Lk1} + \psi^\dagger_{Lk1}\psi_{Lk0} - \psi^\dagger_{Rk0}\psi_{Rk1} - \psi^\dagger_{Rk1}\psi_{Rk0}). \tag{28}$$

Now we make a mean-field approximation ($\varphi=0$) on the terms which contain continuum states Lk', Rk'. Projected onto the discrete basis (L,d,R), $\hat{Y}_1$ then reads

$$\hat{Y}_1 = \varphi\hat{A} + p\hat{B} = \sum_{\beta,\gamma=L,d,R} (\varphi A_{\beta\gamma} + pB_{\beta\gamma}) c^\dagger_\beta c_\gamma. \tag{29}$$

The fermionic operator $\hat{A}$ is represented by a 3×3 matrix $\mathbf{A}$ in $\hat{A}=\Sigma_{\beta\gamma}A_{\beta\gamma}c^\dagger_\beta c_\gamma$ with

$$A_{\beta\gamma} = \frac{\Phi}{2}\sum_k \{a^{Lk}_\beta [g^0_{L\gamma}(\epsilon_{Lk})]^* + g^0_{L\beta}(\epsilon_{Lk})(a^{Lk}_\gamma)^* - a^{Rk}_\beta (g^0_{R\gamma}(\epsilon_{Rk}))^* - g^0_{R\beta}(\epsilon_{Rk})(a^{Rk}_\gamma)^*\}. \tag{30}$$

The matrix $\mathbf{B}$ is obtained similarly with $a^{\alpha k}_\beta$ replaced by $b^{\alpha k}_\beta$ in the above expression. We emphasize that, while the bias operator $\hat{Y}$ is expanded up to the harmonic approximation, the full solution of the effective Hamiltonian $\hat{H}-\hat{Y}$ contains all orders of el-ph interaction.

The noninteracting Matsubara Green function $G^0_{\beta\gamma}(i\omega_n)$ projected on to the discrete basis states is

$$G^0_{\beta\gamma}(i\omega_n) = \sum_{\alpha=L,R;k} \frac{g^0_{\alpha\beta}(\epsilon_{\alpha k})[g^0_{\alpha\gamma}(\epsilon_{\alpha k})]^*}{i\omega_n - \epsilon_{\alpha k} + (-)^\alpha \Phi/2} + \sum_m \frac{c^m_\beta c^{m*}_\gamma}{i\omega_n - E_m}. \tag{31}$$

Here, in the second term, we have included the possible localized states (with the mth discrete energy E_m and the amplitude c^m_β for the state β) outside the continuum in the narrow-band limit. The position of the discrete poles E_m can be identified from sharp peaks in the spectral function of $g^0_d(\epsilon)$ outside the continuum. Since the localized states do not contribute to the transport, there is no chemical potential shift associated with the discrete energy E_m in the energy denominator.

The total effective action can be summarized now as follows:

$$S = -\int_0^\beta d\tau \int_0^\beta d\tau' \sum_{\beta\gamma=d,L,R} c^\dagger_\beta(\tau)[G^0(\tau-\tau')]^{-1}_{\beta\gamma} c_\gamma(\tau') + \frac{1}{2}\int_0^\beta d\tau \left[\left(\frac{d\varphi}{d\tau}\right)^2 + \omega^2_{ph}\varphi^2\right] + \int_0^\beta d\tau \{\alpha\varphi(\tau)[d^\dagger(\tau)d(\tau) - \langle d^\dagger d\rangle] - \varphi(\tau)\hat{A}(\tau) - p(\tau)\hat{B}(\tau)\}, \tag{32}$$

with the nonequilibrium partition function expressed in the path integral[12] $Z_{\text{noneq}}=\int \mathcal{D}[c^\dagger,c]e^{-S}$. We sample the nonequilibrium ensemble by using the finite-temperature QMC (Ref. 5) in the imaginary-time space. We approximate the path integral Eq. (32) by discretizing the Boltzmann factor in the Trotter breakup,[5,13] $\mathrm{Tr}\exp(-\beta\hat{H}_{\text{noneq}})=\mathrm{Tr}[\exp(-\Delta\tau\hat{H}_{\text{noneq}})]^N$ with $\beta=N\Delta\tau$. The three discrete sites (L,d,R) are considered as a generalized impurity in the sense of the Anderson impurity model and the Hirsch-Fye algorithm[13] is employed to integrate out the continuum states.

The main difference of the our effective Hamiltonian from the equilibrium el-ph Hamiltonian is the p term in Eq. (29). Integrating out the canonical momentum p inside a time slice leads to[14]

$$\langle\varphi_{\tau+\Delta\tau}|\exp\left[-\Delta\tau\left(\frac{1}{2}\hat{p}^2 + \hat{p}\hat{B}\right)\right]|\varphi_\tau\rangle \propto \exp\left[\Delta\tau\left\{-\frac{1}{2}\left(\frac{\partial\varphi}{\partial\tau}\right)^2 + i\hat{B}_\tau\frac{\partial\varphi}{\partial\tau}\right\}\right], \tag{33}$$

where $\hat{B}_\tau$ is the electronic operator at the imaginary time τ. Due to the second term $\hat{B}_\tau(\partial\varphi/\partial\tau)$, a temporally local update of the phonon field φ_τ influences the electronic operators $\hat{B}_{\tau-\Delta\tau}$, $\hat{B}_{\tau+\Delta\tau}$ at adjacent times (see Appendix C). The apparent broken time-reversal symmetry in the first-order time differentiation $(\partial\varphi/\partial\tau)$ originates from the source-to-drain flow of electrons induced by the bias Φ.[15] The $(\partial\varphi/\partial\tau)$ term also shows bias-induced phonon fluctuations which become crucial in phonon-assisted tunneling.[17]

Due to the complexity of the Hamiltonian, the path integral of fermionic degree of freedom at a given snapshot of bosonic configuration $\varphi_i[=\varphi(\tau_i)]$ need not be real. Therefore, we factor out the phase $\rho(\{\varphi_i\})/|\rho(\{\varphi_i\})|$ from the path integral of the Boltzmann factor, $\rho(\{\varphi_i\})$, to define the positive definite probability $|\rho(\{\varphi_i\})|$. Then the stochastic average of a physical quantity A is weighted by the phase factor as

$$\langle A\rangle = \sum_{\{\varphi_i\}} A(\{\varphi_i\})\rho(\{\varphi_i\}) = \left\langle\left\langle A(\{\varphi_i\})\frac{\rho(\{\varphi_i\})}{|\rho(\{\varphi_i\})|}\right\rangle\right\rangle, \tag{34}$$

where the $\langle\langle\cdots\rangle\rangle$ average is taken over the Markov chain of phonon configurations $\{\varphi_i\}$ with the probability given by $|\rho(\{\varphi_i\})|$.

The sign-problem[18] often plagues QMC calculations in interacting fermion models due to nonpositive path integrals at fixed auxiliary decoupling fields. In general, the sign problem is expected to become even worse in the form of the phase problem. However, just as the absence of the sign problem in the electron-phonon systems at equilibrium, the phase factors in this calculation turn out to be real, i.e., $\rho(\{\varphi_i\})/|\rho(\{\varphi_i\})|=1$, with error bars far smaller than 1%.

III. RESULTS

I-V curves in the broadband limit ($D\gg\omega_{ph}$) are presented in Fig. 2. The unit of energy is chosen so that the bare phonon level ($\omega_{ph}=0.5$) aligns with the Fermi energy of the L reservoir at the unit bias ($\Phi=1$). The current monotonically increased with Φ at all el-ph coupling constant g. The current converges toward the well-known large-band, large-bias limit (dashed line for $g=0$) (Ref. 19)

$$I = \frac{2e}{\hbar}\frac{\Gamma_L\Gamma_R}{\Gamma_L+\Gamma_R}, \quad \text{with } \Gamma_a = \pi t^2_\alpha N_\alpha(0). \tag{35}$$

The data reported in this paper have the discretization step $\Delta\tau=1$ for the imaginary-time variable. The discretization er-

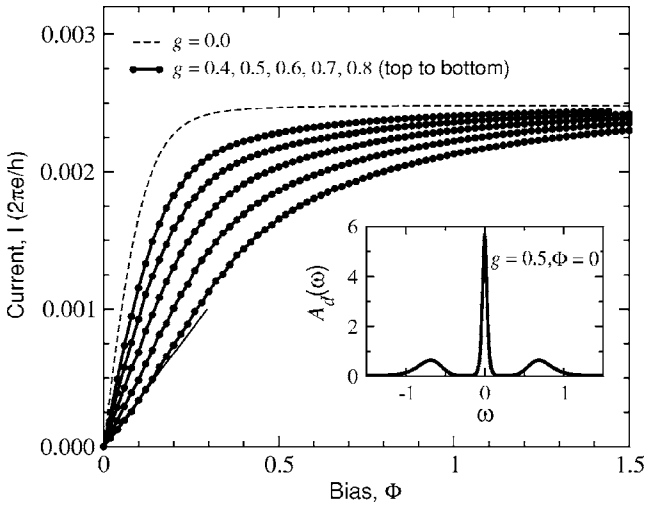

FIG. 2. Simulated *I-V* characteristics in the broadband limit, $D \gg \omega_{ph}$. Parameters are $t_L = t_R = 0.1$, $\omega_{ph} = 0.5$, $D = 8.0$, and $T = 1/32 = 0.03\,125$. The current decreased with increasing electron-phonon coupling constant g. Noninteracting phonon level aligns with the reservoir Fermi energy at the unit bias $\Phi = 2\omega_{ph} = 1$. The phonon dephasing effect is so strong that the phonon satellite peak is invisible at all coupling constant while the phonon satellites at zero bias (inset) are clearly separated from the main peak.

ror estimated at selected sets of data have shown that the current reported here is somewhat overestimated. For the case of the strongest el-ph coupling and lowest temperature ($g = 0.8, T = 1/32$), where we expect the worst discretization error due to the strong electron correlation, the current with $\Delta\tau = 1/2$ showed a maximum discrepancy of 20% reduction. Although the data have not been taken in the $\Delta\tau \to 0$ limit systematically due to computational limitations, the conclusions reported here are robust.

At zero bias, the QD spectral function $A_d(\omega)$ at real frequency ω (see inset of Fig. 2), obtained by using the maximum entropy method,[20] shows that the phonon satellite peaks are clearly separated from the main peak.[21] With this, one might expect that there would be distinctive double-step *I-V* characteristics, which we do not observe in the calculated curves in Fig. 2. This suggests that the actual decay rate of the phonon satellite under finite bias ($\Phi/2 \approx \omega_{ph}$) is significantly larger than at zero bias because the phonon level is now close to a resonance with the reservoir Fermi energy.

However, upon a close inspection of the curves, we find that the line shape changes slightly before the current saturates at large bias. One cannot fit the curves at large g to a one-shoulder curve of the weak coupling limit.[16] To guide the eye, a tangential line is drawn at $g = 0.8$ in the zero bias limit. The initial slope at small bias decreases strongly with the el-ph coupling strength due to the highly renormalized low energy state. As Φ increases, the coherent transport quickly gives way to the incoherent transport which can be characterized by phonon excitations over a broad bias range. In the broadband limit, the dominant role of the phonon is the dephasing effect due to the fluctuation of the QD level $\epsilon_d(\varphi) = \epsilon_d + \alpha\varphi$ via the $\hat{Y}_0$ term, instead of phonon excitations serving as well-defined discrete levels. The current is insensitive to the choice of $\hat{Y}_1$ in the large bandwidth limit.

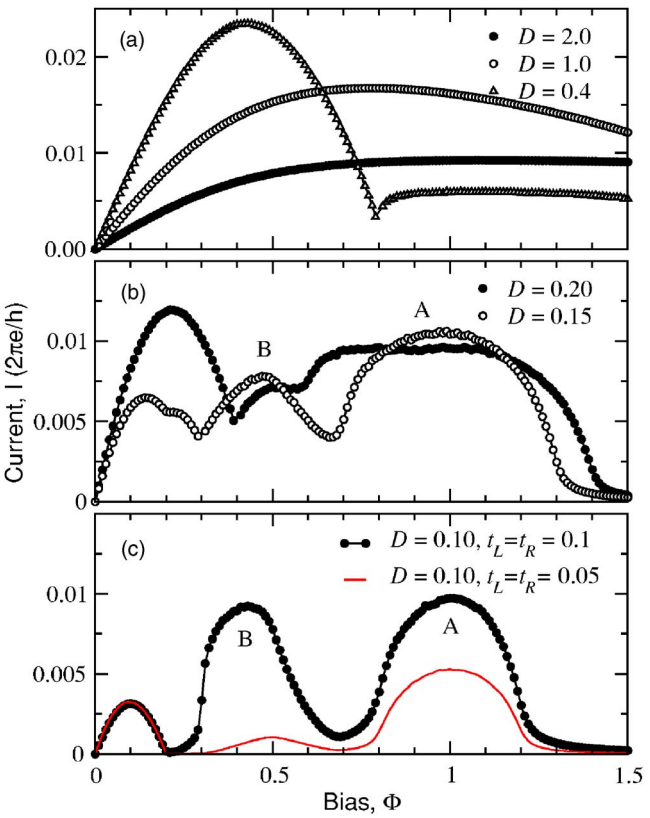

FIG. 3. (Color online) *I-V* characteristics for narrow bandwidth limit. $t_L = t_R = 0.1$ [except for (c)], $\omega_{ph} = 1$, $g = 0.2$, and $T = 1/12 = 0.0833$. (a) The saturated current in the large bandwidth limit gradually turns into negative differential resistance regime as Φ becomes comparable to D. (b). A three-peak structure emerges as D gets further reduced. The peaks correspond to ballistic coherent transport, phonon-assisted tunneling (B, $\Phi = \omega_{ph}$) and sequential off-resonant transport (A, $\Phi = 2\omega_{ph}$). (c) Reduction of tunneling parameter t_L, t_R dramatically suppresses the phonon-assisted tunneling compared to the sequential current.

In the narrow-band limit, one obtains negative differential resistance (NDR) behavior.[17] Figures 3(a)–3(c) show the results as the bandwidth D is gradually decreased. Parameters are $\omega_{ph} = 0.5$, $t_L = t_R = 0.1$ [except for (c) as specified in the figure] and $T = 1/12 = 0.0833$. As D becomes comparable to Φ, a gradual NDR behavior shows up due to the decreasing cross-lead overlap of L,R-DOS. As D is further decreased a distinct discrete three-peak feature emerges as shown in Figs. 3(b) and 3(c). The peak near the zero bias is the coherent current corresponding to the ballistic transport renormalized by the el-ph interaction. As D is reduced well below T, the maximum height of the ballistic current gets reduced due to the thermal dephasing.

The phonon satellite peak at higher bias ($\Phi = 2\omega_{ph} = 1$, marked as A in the plot) becomes evident in Fig. 3(b). The electronic transport in this regime is sequential,[1] i.e., an electron from the L-reservoir tunnels to the QD by emitting a phonon and loses its phase information before it tunnels out to the R reservoir with an emission of another phonon. The width of the structure is twice as large as the full bandwidth,

$4D$, as expected. It is interesting that the phonon structures for $D=0.20$ have the familiar staircase I-V curve, indicating that the phonons start to behave as discrete current channels due to the reduced decay paths to continuum. This is in contrast to the large bandwidth limit where the phonon acts more as a dephaser than as a discrete state. We emphasize that the phonon satellite features A and B are due to the first order correction to $\hat{Y}$, particularly the p term in $\hat{Y}_1$. As can be seen from the energy denominator in Eq. (B9), the bias operator $\hat{Y}_1$ has a strong contribution from energy poles at the phonon frequency due to the reduced damping in the small bandwidth limit. It can be also inferred from Eq. (B9) that if we go to a higher order of perturbation in the el-ph coupling constant, the pole structure in Eq. (B9) will be modified with a shifted phonon frequency and that, more importantly, multiphonon satellites (higher than the second harmonics $\Phi = n\omega_{ph}$, $n>2$) will emerge at energies of roughly integer multiples of the phonon frequency ω_{ph}.

An intriguing feature in the I-V curves is the phonon-assisted tunneling marked as B in Fig. 3. As depicted in Fig. 4, the tunneling happens by the energy exchange between a cross-lead particle-hole pair and a phonon on the QD at the bias $\Phi=\omega_{ph}$. The curves at $D=0.4, 0.2$ resemble the experimental results.[17] This is a direct consequence of the coherence built in the $\hat{Y}$ operator, Eq. (29), and should be distinguished from the sequential tunneling. To demonstrate the point, a calculation with reduced tunneling parameters $t_L = t_R = 0.05$ is shown as a thin (red) line in Fig. 3(c). Since the phonon-assisted tunneling is mediated by a coherent electron-hole pair creation over the whole device, its tunneling amplitude is proportional to the cross-lead overlap $t_L t_R$, while the amplitude for the sequential tunneling is proportional to t_L or t_R separately due to the uncorrelated sequential tunneling events. The much reduced peak B supports the argument.

IV. CONCLUSION

We have formulated a quantum simulation algorithm for steady-state nonequilibrium and have shown that the nonequilibrium can be mapped to an effective equilibrium ensemble through a statistical operator $\hat{Y}$ which imposes the nonequilibrium boundary condition. We have explicitly demonstrated that, in the noninteracting limit, the results from the nonequilibrium ensemble mapping is equivalent to the well-known nonequilibrium Green function technique. As the first application of the method to an interacting case, we have formulated a scheme to construct $\hat{Y}$ in the electron-phonon coupled quantum dot system. We have used the quantum Monte Carlo technique to compute the electric current over the nonequilibrium ensemble and have reproduced the important physics in the system, such as phonon dephasing, phonon-assisted tunneling, and incoherent multiphonon transport. This study suggests that the mapping between nonequilibrium steady state and equilibrium ensembles makes other numerical many-body tools readily applicable to a wide range of nonequilibrium problems. The combination of the effective ensemble method with many-body computational techniques and the existing nonequilibrium Green function technique will provide a critical step toward a more complete theory of steady-state transport.

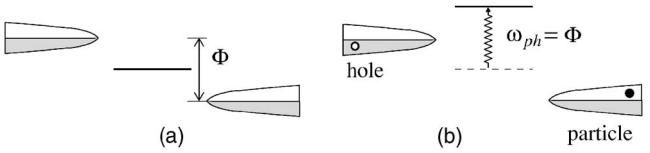

FIG. 4. (a) Initial and (b) final states in the phonon assisted tunneling process. The particle-hole and phonon excitations are resonant at the bias $\Phi=\omega_{ph}$.

This method has a great potential for a wide variety of problems such as strongly correlated transport, transport through disorder at high bias, spin transport. The success of this method critically hinges on the proper construction scheme of the bias operator, and deeper understanding of the bias operator $\hat{Y}$ itself. In this work, we have used perturbative expansion of the interaction within the harmonic approximation of the electron-phonon coupling. However, in the system of strong correlation effects such as in the Kondo anomaly phenomena, more sophisticated unperturbative expansion is expected in order to incorporate the strong correlation effects in the bias operator $\hat{Y}$.

ACKNOWLEDGMENTS

I thank A. Schiller, F. Anders, and P. Bokes for helpful discussions. I acknowledge support from the National Science Foundation DMR-0426826 and computational resources from the Center for Computational Research at SUNY Buffalo.

APPENDIX A: DERIVATION OF CURRENT IN NONINTERACTING LIMIT

As one of the central results in this work, we derive the current in the noninteracting limit within the equilibrium formulation. First, to evaluate the current given in Eq. (2), we define a discrete L state which couples to the QD d level as $c_L^\dagger = \Omega^{-1/2}\Sigma_k c_{Lk}^\dagger$. Therefore, the current expression can be rewritten as

$$I = -\frac{ie}{\hbar} t_L[\langle d^\dagger c_L\rangle - \langle c_L^\dagger d\rangle], \tag{A1}$$

where we have used a k-independent hopping integral t_L for simplicity. The quantity in the square bracket can be written in terms of off-diagonal Matsubara Green functions as

$$I = \frac{ie}{\hbar}\frac{1}{\beta}\sum_n t_L[G_{dL}(i\omega_n) - G_{Ld}(i\omega_n)]. \tag{A2}$$

Following the similar steps as in Eqs. (17)–(19) within the one-body interaction, the off-diagonal Green function $G_{Ld}(i\omega_n)$ can be expanded in terms of scattering states as

$$
\begin{aligned}
&t_L G_{Ld}(i\omega_n) \\
&= t_L\left[\left\langle c_L \frac{1}{i\omega_n - \mathcal{L}_{H-Y}} d^\dagger \right\rangle - \left\langle d^\dagger \frac{1}{-i\omega_n - \mathcal{L}_{H-Y}} c_L \right\rangle\right] \\
&= \frac{t_L}{\sqrt{\Omega}} \sum_{kk'} \left(\frac{\langle c_{Lk}|\psi_{Lk'}\rangle\langle\psi_{Lk'}|d\rangle}{i\omega_n - \epsilon_{Lk'} + \Phi/2} + \frac{\langle c_{Lk}|\psi_{Rk'}\rangle\langle\psi_{Rk'}|d\rangle}{i\omega_n - \epsilon_{Rk'} - \Phi/2} \right) \\
&= \frac{\Gamma_L}{\pi}\Bigg[(2\pi i) g_d^0(i\omega_n + \Phi/2)\,\theta(-n) \\
&\quad + \frac{-i\pi t_L^2}{\Omega} \sum_{k'} \frac{|g_d^0(\epsilon_{Lk'})|^2}{i\omega_n - \epsilon_{Lk'} + \Phi/2} \\
&\quad + \frac{-i\pi t_R^2}{\Omega} \sum_{k'} \frac{|g_d^0(\epsilon_{Rk'})|^2}{i\omega_n - \epsilon_{Rk'} - \Phi/2} \Bigg] \\
&= i\Gamma_L\Bigg[2 g_d^0(i\omega_n + \Phi/2)\,\theta(-n) - \frac{\Gamma_L}{\Gamma} g_d^0(i\omega_n + \Phi/2) \\
&\quad - \frac{\Gamma_R}{\Gamma} g_d^0(i\omega_n - \Phi/2) \Bigg],
\end{aligned}
\tag{A3}
$$

where the step function $\theta(x)$ is defined as 1 for $x>0$ and 0 for $x<0$. The retarded/advanced QD Green function $g_d^0(\epsilon)/[g_d^0(\epsilon)]^*$ has been analytically continued to the whole complex plane in the third and fourth lines above. The first term in the third line is due to the incoming part $c_{Lk}^\dagger$ in the scattering state operator $\psi_{Lk}^\dagger$. In the above calculation, summation over continuum states is replaced by an integral in the large band limit as $\Omega^{-1}\Sigma_k \leftrightarrow N(0)\int d\epsilon$. We can evaluate $t_L G_{dL}(i\omega_n)$ similarly as

$$
\begin{aligned}
t_L G_{dL}(i\omega_n) = i\Gamma_L\Bigg[&- 2 g_d^0(i\omega_n + \Phi/2)\,\theta(n) + \frac{\Gamma_L}{\Gamma} g_d^0(i\omega_n + \Phi/2) \\
&+ \frac{\Gamma_R}{\Gamma} g_d^0(i\omega_n - \Phi/2) \Bigg].
\end{aligned}
\tag{A4}
$$

The current expression, Eq. (A2), becomes

$$
I = \frac{e}{\hbar}\frac{1}{\beta}\sum_n \frac{2\Gamma_L\Gamma_R}{\Gamma_L + \Gamma_R}[g_d^0(i\omega_n + \Phi/2) - g_d^0(i\omega_n - \Phi/2)],
\tag{A5}
$$

in agreement with Eq. (22). Using the spectral representation of the Green function $g_d^0(z)$ in

$$
g_d^0(z) = \int d\epsilon \frac{\rho(\epsilon)}{z - \epsilon}, \quad \text{with } \rho(\epsilon) = \frac{\Gamma/\pi}{(\epsilon - \epsilon_d)^2 + \Gamma^2},
\tag{A6}
$$

we obtain

$$
\begin{aligned}
I &= \frac{2e}{\hbar}\frac{\Gamma_L\Gamma_R}{\Gamma_L + \Gamma_R}\frac{1}{\beta}\sum_n \int d\epsilon \rho(\epsilon) \\
&\quad \times \left(\frac{1}{i\omega_n + \Phi/2 - \epsilon} - \frac{1}{i\omega_n - \Phi/2 - \epsilon} \right) \\
&= \frac{2e}{\hbar}\frac{\Gamma_L\Gamma_R}{\Gamma_L + \Gamma_R} \int d\epsilon \rho(\epsilon)[f(\epsilon - \Phi/2) - f(\epsilon + \Phi/2)].
\end{aligned}
\tag{A7}
$$

APPENDIX B: FIRST ORDER EXPANSION $\psi_{\alpha k,1}$ WITH el-ph INTERACTION

By substituting $\psi_0^\dagger$ and $\psi_1^\dagger$ in Eqs. (26) and (27) into the recursion relation Eq. (24) with $n=1$, $[\hat{H}_{\rm ep}, \psi_{Lk,0}^\dagger] = (\epsilon_{Lk} + i\eta)\psi_{Lk,1}^\dagger - [\hat{H}_0, \psi_{Lk,1}^\dagger]$, we obtain relations

$$
a_{Lk'} = \Delta_{Lk'}^{-1}\left(i\omega_{ph}^2 b_{Lk'} + \frac{t_0}{\sqrt{\Omega}} a_L \right),
\tag{B1}
$$

$$
a_L = \Delta_L^{-1}\left(i\omega_{ph}^2 b_L + \frac{t_0}{\sqrt{\Omega}} \sum_{k''} a_{Lk''} + t_L a_d \right),
\tag{B2}
$$

$$
a_d = \Delta_d^{-1}\left[\frac{t_0\alpha}{\sqrt{\Omega}} g_{Ld}^0(\epsilon_{Lk}) + i\omega_{ph}^2 b_d + t_L a_L + t_R a_R \right],
\tag{B3}
$$

$$
a_R = \Delta_R^{-1}\left(i\omega_{ph}^2 b_R + \frac{t_0}{\sqrt{\Omega}} \sum_{k''} a_{Rk''} + t_R a_d \right),
\tag{B4}
$$

$$
a_{Rk'} = \Delta_{Rk'}^{-1}\left(i\omega_{ph}^2 b_{Rk'} + \frac{t_0}{\sqrt{\Omega}} a_R \right),
\tag{B5}
$$

with $\Delta_\beta = \epsilon_{Lk} - \epsilon_\beta + i\eta$. The superscripts Lk in a_β^{Lk}, b_β^{Lk} in Eq. (27) have been suppressed. In the derivation, we have used the commutation relations, $[\hat{H}_{\rm ph}, \varphi] = -ip$ and $[\hat{H}_{\rm ph}, p] = i\omega_{ph}^2\varphi$. Relations for b_β can be obtained by switching a_β and $i\omega_{ph} b_\beta$ in the above equations except for $\beta = d$. b_d is given as

$$
b_d = \Delta_d^{-1}(-ia_d + t_L b_L + t_R b_R).
\tag{B6}
$$

After summing over the continuum states, we reduce Eqs. (B1), (B2), (B4), and (B5) to

$$(\Delta_L - t_0^2 I_L^0) a_L = i\omega_{ph}^2 (1 + t_0^2 I_L^1) b_L + t_L a_d, \tag{B7}$$

$$(\Delta_R - t_0^2 I_R^0) a_R = i\omega_{ph}^2 (1 + t_0^2 I_R^1) b_R + t_R a_d. \tag{B8}$$

where

$$I_\alpha^0 = \frac{1}{\Omega} \sum_{k'} \frac{1}{(\epsilon_{Lk} - \epsilon_{\alpha k'} + i\eta)^2 - \omega_{ph}^2}$$

and

$$I_\alpha^1 = \frac{1}{\Omega} \sum_{k'} \frac{\epsilon_{Lk} - \epsilon_{\alpha k'}}{(\epsilon_{Lk} - \epsilon_{\alpha k'} + i\eta)^2 - \omega_{ph}^2}. \tag{B9}$$

Similar equations relating b_d to a_L, a_R, b_L, b_R are

$$(\Delta_L - t_0^2 I_L^0) b_L = -i(1 + t_0^2 I_L^1) a_L + t_L b_d, \tag{B10}$$

$$(\Delta_R - t_0^2 I_R^0) b_R = -i(1 + t_0^2 I_R^1) a_R + t_R b_d. \tag{B11}$$

We obtain explicit expressions for a_d, a_L, a_R, b_d, b_L, b_R by solving the six closed Eqs. (B3), (B6)–(B8), (B10), and (B11).

APPENDIX C: INTEGRATION OF CONJUGATE MOMENTUM

The mapping of the electron-phonon interaction in the steady-state nonequilibrium creates an interaction term proportional to the phonon conjugate momentum, $p\hat{B}$ in Eq. (29). This term is proportional to the bias Φ. Since we perform the QMC sampling with respect to the coherent phonon states parametrized by the phonon amplitude φ,[14] we integrate out the conjugate momentum p as follows:

$$\begin{aligned}
&\langle \varphi_{\tau+\Delta\tau} | e^{-\Delta\tau(1/2\ \hat{p}^2 + \hat{p}\hat{B})} | \varphi_\tau \rangle \\
&= \int \frac{dp}{2\pi} \langle \varphi_{\tau+\Delta\tau} | p \rangle e^{-\Delta\tau(1/2\ p^2 + p\hat{B})} \langle p | \varphi_\tau \rangle \\
&= \int \frac{dp}{2\pi} e^{ip(\varphi_1 - \varphi_2) - \Delta\tau(1/2\ p^2 + p\hat{B})} \\
&\propto \exp\left[-\frac{\Delta\tau}{2} \left(\frac{\Delta\varphi^2}{\Delta\tau^2} + 2i\hat{B}\frac{\Delta\varphi}{\Delta\tau} - \hat{B}^2 \right) \right],
\end{aligned} \tag{C1}$$

with $\Delta\varphi = \varphi_{\tau+\Delta\tau} - \varphi_\tau$. Since the $\hat{B}^2$ term is independent of the phonon fields and proportional to higher order of the el-ph constant α, we ignored the last term. Then the phonon contribution to the Lagrangian can be expressed as

$$L_{\rm ph} = \frac{1}{2}\left(\frac{d\varphi}{d\tau}\right)^2 + \frac{1}{2}\omega_{ph}^2 \varphi^2 + \alpha\varphi(d^\dagger d - \langle d^\dagger d \rangle) - \varphi\hat{A} + i\hat{B}\frac{d\varphi}{d\tau}. \tag{C2}$$

We emphasize that the $i\hat{B}d\varphi/d\tau$ is imaginary with the broken time-reversal symmetry, even if the original Hamiltonian is written in parameters of real numbers. The $i\hat{B}d\varphi/d\tau$ term becomes dominant in the narrow-band limit and is crucial for the nonvanishing current. Since we update the phonon field $\varphi(\tau)$ with temporally local changes in the Monte Carlo sampling, it is convenient to rewrite the $d\varphi/d\tau$ as

$$\begin{aligned}
&\delta \sum_n i\hat{B}(\tau_n) \frac{\varphi(\tau_{n+1}) - \varphi(\tau_{n-1})}{2\Delta\tau} \Bigg|_{\varphi(\tau_m) \to \varphi(\tau_m) + \delta\varphi_m} \\
&= -\frac{i}{2\Delta\tau} \delta\varphi_m [\hat{B}(\tau_{m+1}) - \hat{B}(\tau_{m-1})].
\end{aligned} \tag{C3}$$

[1] S. Datta, *Electronic Transport in Mesoscopic Systems* (Cambridge University Press, Cambridge, UK, 1995).
[2] J. Rammer and H. Smith, Rev. Mod. Phys. **58**, 323 (1986).
[3] N. S. Wingreen, K. W. Jacobsen, and J. W. Wilkins, Phys. Rev. Lett. **61**, 1396 (1988); N. S. Wingreen, K. W. Jacobsen, and J. W. Wilkins, Phys. Rev. B **40**, 11834 (1989).
[4] R. Lake and S. Datta, Phys. Rev. B **45**, 6670 (1992).
[5] R. Blankenbecler, D. J. Scalapino, and R. L. Sugar, Phys. Rev. D **24**, 2278 (1981).
[6] D. N. Zubarev, *Nonequilibrium Statistical Thermodynamics* (Consultants Bureau, New York, 1974).
[7] S. Hershfield, Phys. Rev. Lett. **70**, 2134 (1993).
[8] In the narrow-band limit or band with a sharp edge, there are localized states which cannot be included in $\psi_{\alpha k\sigma}$. However, they do not contribute to $\hat{Y}$.
[9] Eugen Merzbacher, *Quantum Mechanics* (Wiley, New York, 1961).
[10] A. Schiller and S. Hershfield, Phys. Rev. B **51**, 12896 (1995).
[11] P. Bokes and R. W. Godby, Phys. Rev. B **68**, 125414 (2003).
[12] R. P. Feynmann and A. R. Hibbs, *Quantum Mechanics and Path Integrals* (McGraw-Hill, New York, 1965).
[13] R. M. Fye and J. E. Hirsch, Phys. Rev. B **38**, 433 (1988).
[14] J. W. Negele and H. Orland, *Quantum Many-Particle Systems* (Addison-Wesley, New York, 1988).
[15] D. E. Feldman, Phys. Rev. Lett. **95**, 177201 (2005).
[16] The low bias shoulder ($\Phi \sim 0.2$) becomes slightly more pronounced at smaller discretization step, $\Delta\tau = 0.5$. At higher bias, the discretization error becomes smaller due to the saturation of current, Eq. (35).
[17] V. J. Goldman, D. C. Tsui, and J. E. Cunningham, Phys. Rev. Lett. **58**, 1256 (1987).
[18] E. Y. Loh, Jr., J. E. Gubernatis, R. T. Scalettar, S. R. White, D. J. Scalapino, and R. L. Sugar, Phys. Rev. B **41**, 9301 (1990).
[19] This expression does not include summation over spins.
[20] M. Jarrell and J. E. Gubernatis, Phys. Rep. **269**, 2278 (1981).
[21] Direct analytic continuation at finite bias does not have an obvious physical meaning since the Green functions [see Eq. (31)] have poles from $\hat{H} - \hat{Y}$, not $\hat{H}$.